Exchange of stability in Cattaneo - LTNE porous convection

B. Straughan
Department of Mathematics
University of Durham, DH1 3LE, U.K.

April 12, 2015

Abstract

We investigate a problem of convection in local thermal non - equilibrium (LTNE) porous media. This is where the solid skeleton and the fluid may have different temperatures. However, due to increasing interest in thermal wave motion, especially at micro - nano - scales and particularly in solids, we analyse a model for thermal convection in a fluid saturated Darcy porous medium allowing the solid and fluid parts to be at different temperatures. This theory employs thermodynamics for the fluid based on Fourier's law of heat conduction, whereas for the solid skeleton heat is transferred by means of the Cattaneo heat flux theory. Under appropriate conditions oscillatory convection is found whereas for the standard LTNE Darcy model this does not exist. In this article we concentrate on a transition which is found when the heat transfer interaction coefficient reaches a critical level and this leads to an exchange of stability for a certain porosity level.

1 Introduction

Thermal convection in a saturated porous medium is a subject of immense current interest. In recent work particular interest has focussed attention on thermal convection in a porous medium where the fluid temperature, T_f, may be different from the solid skeleton temperature, T_s. The phenomenon where the two temperatures may be different is usually referred to as local thermal non-equilibrium, usually abbreviated to LTNE. Perhaps the main reason for the increased attention of LTNE flows in porous media is due to the large number of applications of this area in real life. As Straughan [24], section 1.1.1 and Straughan [23] cites, there are applications to tube refrigerators in space, to nanofluid flows, in fuel cells, in resin flow in composite materials production, in nuclear reactor maintenance, in heat exchangers, in flows in microchannels, in flow in porous metallic foams, in textile transport, in convection in stellar

atmospheres, and in many other areas. References to this work may be found in Straughan [24], section 1.1.1 and Straughan [23].

Continuum theories for local thermal non-equilibrium effects on flow in porous materials appear to have been introduced in the late 1990's, cf. the work of Nield [14], Minkowycz *et al.* [13], and Petit *et al.* [16]. Instability giving rise to thermal convective motion involving LTNE effects was analysed by Banu & Rees [4], by Malashetty *et al.* [12], and by Straughan [21]. Straughan [23] coupled LTNE theory together with hyperbolic heat flow in the solid skeleton and developed a theory for thermal convection in a porous medium. We believe this is important because modern technology is leading to the creation of smaller and smaller devices, and then the phenomenon of temperature travelling as a wave becomes increasingly important, especially in metallic like solids. In particular, Pilgrim *et al.* [17] note that, ... the "hyperbolic description will become increasingly important as device dimensions move even further into the deep sub-micron regime". Many further articles emphasizing the need to consider hyperbolic heat transport in nanowires and in thin films are cited in Straughan [22] and in Straughan [24], and further recent relevant work with finite propagation speed heat waves may be found in Christov & Jordan [6], Fabrizio & Lazzari [8], Franchi *et al.* [9, 10], Papanicolaou *et al.* [15]. The model of Straughan [23] utilized Darcy's law to describe flow in the porous medium and a very interesting extension to use Brinkman theory is by Shivakumara *et al.* [20]. This paper includes a detailed analysis of instability using their Brinkman - Cattaneo - LTNE theory.

The goal of this work is to extend the instability analysis of Straughan [23] and Straughan [24], section 15.4. In particular we note that Straughan [24], section 15.4, employs various materials for the solid skeleton and observes that the type of instability which may instigate thermal convection, stationary or oscillatory convection, may depend on the porosity of the porous medium. In fact, in Straughan [24], figures 15.7, 15.10 and 15.12, he notes that for a porosity ϵ "small" stationary convection may dominate with small convection cells for a thermal interaction coefficient H below a threshold, whilst for ϵ larger oscillatory convection will ensue with small convection cells. The numerical work of Straughan [24], section 15.4, chooses only two porosity values and in this paper we investigate in detail the cell behaviour as the porosity changes. To investigate variation of porosity is not artificial since today porous foams are routinely manufactured and thus one may design a porous medium with a specified porosity.

2 Local thermal non-equilibrium model

The model is derived by Straughan [23] and combines the basic equations for thermal convection in a porous medium with LTNE effects together with a modification of the equation for the solid temperature to allow the heat flux to satisfy a Cattaneo law. The basic system of equations derived by Straughan

[23] (see also section 15.4 of Straughan [24]) is

$$
\begin{aligned}
& v_i = -\frac{K}{\mu}\frac{\partial p}{\partial x_i} + \frac{\rho_f g \alpha K}{\mu} T_f k_i, \\
& \frac{\partial v_i}{\partial x_i} = 0, \\
& (1-\epsilon)(\rho c)_s \frac{\partial T^s}{\partial t} = -\frac{\partial Q_i}{\partial x_i}(1-\epsilon) - h(T_s - T_f), \\
& \tau_s \frac{\partial Q_i}{\partial t} = -Q_i - k_s \frac{\partial T}{\partial x_i}\,, \\
& \epsilon(\rho c)_f \frac{\partial T^f}{\partial t} + (\rho c)_f v_i \frac{\partial T^f}{\partial x_i} = \epsilon k_f \Delta T^f + h(T_s - T_f)\,.
\end{aligned}
\tag{1}
$$

In these equations x_i and t denote space and time, v_i, p, T^s, Q_i, T^f denote fluid (pore averaged) velocity, pressure, solid temperature, heat flux in the solid, and fluid temperature, respectively. The terms $K, \mu, g, \alpha, \epsilon, \rho, c, h, k_s, k_f, \tau_s$ denote permeability, fluid dynamic viscosity, gravity, fluid expansion coefficient, porosity, density, specific heat at constant pressure, a thermal interaction coefficient, thermal conductivity of the solid, thermal conductivity of the fluid, and solid thermal relaxation time, respectively. The notation sub or superscript s or f refers to solid or fluid and Δ is the Laplace operator in 3 - dimensions. Throughout we use standard indicial notation together with the Einstein summation convention, and $\mathbf{k}$ is the vector $\mathbf{k} = (0, 0, 1)$.

Equation $(1)_1$ is Darcy's law, while $(1)_2$ represents conservation of mass. Equation $(1)_3$ is the energy balance equation in the solid, and equation $(1)_4$ represents Cattaneo's law for the solid heat flux. Finally, equation $(1)_5$ is the energy balance equation for the fluid.

The system of equations (1) hold in the layer $\mathbb{R}^2 \times \{z \in (0, d)\}$ with gravity acting in the negative $z-$direction. Due to the fact that Darcy's law is employed the boundary conditions considered are

$$
\begin{aligned}
& v_3 = 0 \text{ on } z = 0, d \qquad \text{and} \\
& T_f = T_s = T_L\,,\ z = 0; \qquad T_f = T_s = T_U\,,\ z = d;
\end{aligned}
\tag{2}
$$

where T_l, T_U are constants with $T_L > T_U$. The steady solution in whose stability we are interested is

$$
\bar{v}_i \equiv 0, \quad \bar{T}_f = \bar{T}_s = -\beta z + T_L\,, \quad \bar{\mathbf{Q}} = (0, 0, k_s \beta). \tag{3}
$$

Here β is the temperature gradient, namely

$$
\beta = \frac{T_L - T_U}{d}\,,
$$

and the steady pressure field, $\bar{p}(z)$, may be found from $(1)_1$.

To study instability of solution (3) Straughan [23] introduces perturbations $(u_i, \pi, \theta, q_i^s, \phi)$ to the steady state $(\bar{v}_i, \bar{p}, \bar{T}^f, \bar{Q}_i, \bar{T}^s)$, and non-dimensionalizes

with the length, time, velocity, pressure, and heat scales $L = d, \mathcal{T} = (\rho c)_f d^2/k_f, U = \epsilon k_f/(\rho c)_f d, P = \mu d U/K$, and $Q^s = k_s T^\sharp/d$. Here $T^\sharp$ is the temperature scale, $T^\sharp = U\sqrt{c_f \beta d^2 \mu/\epsilon k_f g \alpha K}$. Straughan [23] introduces the Rayleigh number $Ra = R^2$, and the non-dimensional coefficients H, A, γ and $\hat{\tau}$ by

$$Ra = R^2 = \frac{\rho_f^2 c_f \beta d^2 K g \alpha}{\mu \epsilon k_f}, \qquad H = \frac{h d^2}{\epsilon k_f},$$
$$A = \frac{(\rho c)_s}{(\rho c)_f}, \qquad \gamma = \frac{\epsilon}{1-\epsilon}, \qquad \hat{\tau} = \frac{\tau_s \kappa_f}{d^2}$$

where $\kappa_f = k_f/\rho_f d^2$. The non-dimensional nonlinear system of perturbation equations derived by Straughan [23] is

$$\begin{aligned}
&u_i = -\frac{\partial \pi}{\partial x_i} + R\theta\, k_i, \\
&\frac{\partial u_i}{\partial x_i} = 0, \\
&\frac{\partial \theta}{\partial t} + u_i \frac{\partial \theta}{\partial x_i} = Rw + \Delta\theta + H(\phi - \theta), \\
&A\frac{\partial \phi}{\partial t} = -\frac{\partial q_i^s}{\partial x_i} - \gamma H(\phi - \theta), \\
&\hat{\tau}\frac{\partial q_i^s}{\partial t} = -q_i^s - \frac{\partial \phi}{\partial x_i}.
\end{aligned} \tag{4}$$

In equation $(4)_3$ w is defined by $w = u_3$.

Equations (4) hold on the domain $\{(x,y) \in \mathbb{R}^2\} \times \{z \in (0,1)\} \times \{t > 0\}$. The perturbation boundary conditions are

$$w = 0, \theta = 0, \phi = 0, \qquad z = 0, 1, \tag{5}$$

and $(u_i, \pi, \theta, \phi, q_i^s)$ satisfy a plane tiling periodicity in the (x,y) plane.

3 Linear instability

To investigate instability Straughan [23] discards the nonlinear term in equation $(4)_3$, takes curlcurl of equation $(4)_1$ and retains the third component. He then seeks a time dependence like $e^{\sigma t}$ and then using the boundary conditions (5) he develops a $\sin n\pi z$ series solution. He shows that the stationary convection boundary is found from the equation

$$R^2_{stat} = \frac{\Lambda^3 + \Lambda^2(1+\gamma)H}{a^2(\Lambda + \gamma H)}, \tag{6}$$

where a is a wavenumber and $\Lambda = n^2\pi^2 + a^2$. In fact, the stationary convection boundary is found for fixed γ and H by minimizing R^2_{stat} in a^2 with $n = 1$.

The oscillatory convection boundary arises from the two equations

$$\begin{aligned} &-\hat{\tau}A\Lambda\sigma_1^2+\Lambda[\gamma H+\Lambda A+HA+\hat{\tau}\gamma H\Lambda+\Lambda]=R^2a^2(\hat{\tau}\gamma H+A),\\ &-\Lambda\big[\hat{\tau}(\gamma H+\Lambda A+HA)+A\big]\sigma_1^2+\Lambda^2[\gamma H+\Lambda+H]\\ &\qquad\qquad=R^2a^2[-\hat{\tau}A\sigma_1^2+\Lambda+\gamma H], \end{aligned} \tag{7}$$

where σ_1 is the imaginary part of the growth rate σ. Straughan [23] shows that the oscillatory convection boundary is determined from the expression

$$R^2_{osc}=\frac{1}{a^2}\left(\frac{b-\sqrt{b^2-4Xc}}{2X}\right). \tag{8}$$

In addition, σ_1^2 is given by

$$\sigma_1^2=\frac{H}{\hat{\tau}}\Big(\frac{\gamma}{A}+1\Big)+\frac{\Lambda}{A\hat{\tau}}\,(1+k_1)-R^2a^2\frac{k_1}{A\hat{\tau}\Lambda}\,. \tag{9}$$

In equations (8) and (9) the relevant terms are given by

$$\begin{aligned} &X=\frac{k_1}{\Lambda}\,,\qquad b=2k_1\Lambda+k_2\,,\\ &c=k_1\Lambda^3+\left(k_2+\frac{k_1}{A\hat{\tau}}\right)\Lambda^2+\Lambda H\left[2\gamma H+\frac{\gamma^2H}{A}+AH+\frac{(\gamma+A)}{\hat{\tau}}\right], \end{aligned}$$

with k_1 and k_2 given by

$$k_1=A+\hat{\tau}\gamma H,\qquad k_2=\frac{k_1^2}{\hat{\tau}A}+k_1H+HA.$$

The oscillatory convection threshold is found by minimizing R^2_{osc} in a^2, comparing with the minimum of R^2_{stat}, and checking with (9) whether $\sigma_1^2>0$ or not.

Numerical results are reported in section 4 where we concentrate on a transition, in the wave number, which is strongly porosity dependent.

4 Numerical results and conclusions

To find the individual terms comprising the coefficient A we employ values from Abid *et al.* [1], Accuratus [2], Aegis Ceramics [3], Boomsma *et al.* [5], Engineering Toolbox [7], and Huisseune *et al.* [11] to calculate values of A. We employ three different types of porous materials and these are Sander sandstone, Abid *et al.* [1], Aluminium Oxide, Al_2O_3, Accuratus [2], and a porous metallic foam, $AL1050$, Huisseune *et al.* [11], and each is saturated with water. The values of $\hat{\tau}$ are chosen as 0.1 and 1. Values for the thermal interaction coefficient are somewhat elusive to obtain, but two excellent papers of Rees [18, 19] indicate how to obtain suitable values for a variety of porous skeleton geometries.

Following Straughan [23], Straughan [24], section 15.4, we find that stationary convection occurs after a transition, the actual transition value of H

depending on the porosity value, for a given porous material and saturating fluid. This behaviour is seen in figures 1 - 4 for a porous skeleton of $AL1050$ saturated with water. Table 4 gives numerical values for the transitions seen in figures 1 - 8. Further detail for $AL1050$ may be found in table 1 and tables 2 and 3 give details for Sander sandstone and aluminium oxide, respectively. The same pattern of transition is observed for all three of the porous materials employed here.

Our main interest is in the wavenumber transitions which may be seen in figures 5 - 8. For example, in figure 5 we observe that when $\epsilon = 0.4$, for H less than the transition value $H_{trans} = 6.89$, instability is by stationary convection whereas it changes to oscillatory convection for $H > H_{trans}$. Just before the transition value of H the wavenumber for stationary convection is larger than the wavenumber for oscillatory convection just after the transition. This means that the cell aspect ratio with $H < H_{trans}$ is smaller than that for $H > H_{trans}$ (both very close to transition). Thus the cell changes from being narrower to wider as oscillatory convection commences. When we examine figure 8 exactly the opposite effect is true. With $\epsilon = 0.95$ the stationary convection cells are wider before H_{trans} and oscillatory convection takes over after H_{trans} with narrower cells.

Since one may produce a particular porosity for many modern materials it is of interest to analyse what happens as H changes from a relatively small value through the transition to a relatively large value, with variation of porosity ϵ. In fact, figure 6 shows that as ϵ increases there is a point at which the stationary convection wavenumber exactly matches the oscillatory convection wavenumber. Details of the behaviour of Ra, a^2 and σ_1^2 (where σ_1 is the imaginary part of the growth rate σ) are given in tables 1 - 3 for three types of saturated porous materials. Each shows the same trend. One begins with a situation like figure 5 in which $a_{stat}^2 > a_{osc}^2$ for ϵ below a transition value and then there is a transition value in ϵ at which $a_{stat}^2 = a_{osc}^2$. Once ϵ exceeds this value $a_{stat}^2 < a_{osc}^2$, with H close to its transition value. Once ϵ increases a little further beyond its transition value we reach a minimum value for H_{trans}. Figure 7 depicts this for $AL1050$ - water, to 2 decimal places in ϵ.

Tables 1 - 3 all indicate that as ϵ approaches its transition value, $\sigma_1^2 \to 0$. This is in complete agreement with the theory. To see this note that at criticality from equation (6) we have

$$R^2 a^2 (\Lambda + \gamma H) = \Lambda^3 + \Lambda^2 (1 + \gamma) H.$$

If we substitute this equation into equation $(7)_2$ then $\sigma_1^2 = 0$ is absolutely consistent.

Another noteable fact we found numerically is that when ϵ becomes close to 1 stationary convection appears to occur always, no matter how large H is. For example, for the $AL1050$ - water material, table 1, we found that with $\epsilon = 0.96$, $Ra_{stat} < Ra_{osc}$. We allowed H to reach 10^6 and Ra_{stat} and Ra_{osc} appear to asymptote to constant values with stationary convection dominant. For Sander sandstone, table 2, with $\epsilon = 0.8$ we found the same effect, that

stationary convection dominates. When Al_2O_3 - water is used we found that with $\epsilon = 0.96$ stationary convection is always observed.

We have found that for a local thermal non-equilibrium porous convection model with Cattaneo effects in the skeleton there is an interesting dependence on porosity regarding cell sizes and stationary or oscillatory convection. For smaller porosities the switch from stationary to oscillatory convection is accompanied by a transition from narrow stationary convection to wider oscillatory convection cells. As the porosity increases the difference between cell sizes decreases until at a critical value of the porosity the stationary convection and oscillatory convection cells have the same size. Thereafter, as the porosity is increased the transition is such that it is from wider stationary convection cells to narrower oscillatory convection cells. The value of the thermal interaction coefficient H decreases as the porosity is increased but it does not achieve a minimum when $Ra_{stat} = Ra_{osc}$ and $a_{stat} = a_{osc}$. The minimum in H is for a porosity slightly greater then the H value when the Rayleigh and wave numbers are equal.

References

[1] M. Abid, U. Hammerschmidt, and J. Köhler. Temperature and moisture dependent thermophysical properties of Sander sandstone. *Int. J. Thermal Sciences*, 86:88–94, 2014.

[2] Accuratus, 2009. http://www.accuratus.com/alumox.html.

[3] Aegis-Ceramics, 2014. http://www.aegis-ceramics.co.uk/foamet.htm.

[4] N. Banu and D. A. S. Rees. Onset of Darcy-Bénard convection using a thermal non-equilibrium model. *Int. J. Heat Mass Transfer*, 45:2221–2228, 2002.

[5] K. Boomsma, D. Poulikakos, and F. Zwick. Metal foams as compact high performance heat exchangers. *Mechanics of Materials*, 35:1161–1176, 2003.

[6] I. C. Christov, and P. M. Jordan. On an instability exhibited by the ballistic - diffusive heat conduction model of Xu and Hu. *Proc. Royal Soc. London A*, 470:20130557, 2014.

[7] EngineeringToolbox, 2009. http://www.engineeringtoolbox.com/water-thermal-properties-d_162.html.

[8] M. Fabrizio, and B. Lazzari. Stability and second law of thermodynamics in dual - phase - lag heat conduction. *Int. J. Heat Mass Transfer*, 74:484–489, 2014.

[9] F. Franchi, B. Lazzari, and R. Nibbi. The J-S model versus a non ideal MHD theory. *Physics Letters A*, 379:1431–1436, 2015.

[10] F. Franchi, B. Lazzari, and R. Nibbi. Johnson - Segelman viscoelasticity in porous media: stability and wave propagation. *Math. Meth. Appl. Sci.*, Doi: 10.1002/mma.3348.

[11] H. Huisseune, P. De Jaeger, S. De Schampheleire, B. Ameel, and M. De Paepe. Simulation of an aluminium foam heat exchanger using the volume averaging technique. *Procedia Materials Science*, 4:334–339, 2014.

[12] M. S. Malashetty, I. S. Shivakumara, and S. Kulkarni. The onset of Lapwood-Brinkman convection using a thermal non-equilibrium model. *Int. J. Heat Mass Transfer*, 48:1155–1163, 2005.

[13] W. J. Minkowycz, A. Haji-Sheikh, and K. Vafai. On the departure from local thermal non-equilibrium in porous media due to a rapidly changing heat source: the Sparrow number. *Int. J. Heat Mass Transfer*, 42:3373–3385, 1999.

[14] D. A. Nield. Effects of local thermal non-equilibrium in steady convection processes in saturated porous media: forced convection in a channel. *J. Porous Media*, 1:181–186, 1998.

[15] N. C. Papanicolaou, C. I. Christov, and P. M. Jordan. The influence of thermal relaxation on the oscillatory properties of two-gradient convection in a vertical slot. *European Journal of Mechanics B/Fluids*, 30:68–75, 2011.

[16] F. Petit, F. Fichot, and M. Quintard. écoulement diphasique en milieu poreux: modèle à non-équilibre local. *Int. J. Thermal Sciences*, 38:239–249, 1999.

[17] N. J. Pilgrim, W. Batty, R. W. Kelsall, and C. M. Snowden. Nanoscale electrothermal co-simulation: compact dynamic models of hyperbolic heat transport and self-consistent device Monte Carlo. *Microelectronics Journal*, 35:823–830, 2004.

[18] D. A. S. Rees. Microscopic modelling of the two - temperature model for conduction in heterogeneous media: three-dimensional media. In *Proc. 4th International Conference on Applications of Porous Media, Istanbul*, volume 13, pages 125–143, 2009.

[19] D. A. S. Rees. Microscopic modelling of the two - temperature model for conduction in heterogeneous media. *J. Porous Media*, 13:125–143, 2010.

[20] I. S. Shivakumara, M. Ravisha, C. O. Ng, and V. L. Varun. A thermal non-equilibrium model with Cattaneo effect for convection in a Brinkman porous layer. *Int. J. Non-Linear Mech.*, 71:39–47, 2015.

[21] B. Straughan. Global nonlinear stability in porous convection with a thermal non-equilibrium model. *Proc. Roy. Soc. London A*, 462:409–418, 2006.

[22] B. Straughan. *Heat waves*, volume 177 of *Appl. Math. Sci.* Springer, New York, 2011.

[23] B. Straughan. Porous convection with local thermal non-equilibrium effects and Cattaneo effects in the solid. *Proc. Roy. Soc. London A*, 469:201301187, 2013.

[24] B. Straughan. *Convection with local thermal non-equilibrium and microfluidic effects*, volume 32 of *Advances in Mechanics and Applied Mathematics*. Springer, New York, 2015.

ϵ	H_{trans}	a^2_{stat}	a^2_{osc}	σ^2_1	Ra
0.2	10.00	13.222	8.176	6.367	56.09
0.4	6.89	11.906	9.730	0.9747	50.233
0.6	5.17	11.106	10.267	0.1095	46.74
0.8	4.16	10.451	10.373	0.5344×10^{-2}	43.95
0.82	4.122	10.3843	10.3752	0.6184×10^{-3}	43.675
0.822279	4.1193	10.3766	10.3753	0.3336×10^{-6}	43.643221
0.83	4.116	10.3505	10.3757	0.3650×10^{-3}	43.533
0.84	4.121	10.3163	10.3761	0.7884×10^{-3}	43.389
0.85	4.14	10.281	10.376	0.1640×10^{-2}	43.244
0.9	4.72	10.096	10.375	0.5703×10^{-2}	42.468
0.95	95.4	9.875	10.372	0.1260×10^{-1}	41.534

Table 1: Transition critical values of H together with Ra for various values of ϵ. Porous material $AL1050$ saturated with water. Here $A = 0.568407543$ and $\hat{\tau} = 1$.

ϵ	H_{trans}	a^2_{stat}	a^2_{osc}	σ^2_1	Ra
0.15	57.9	17.670	14.210	8.625	108.76
0.2	52.6	15.930	14.490	1.608	98.21
0.24	50.04	14.889	14.615	0.6927×10^{-1}	91.96
0.245	49.80	14.774	14.627	0.2498×10^{-1}	91.28
0.250	49.576	14.661	14.638	0.4989×10^{-2}	90.606
0.251	49.5327	14.6392	14.6397	0.3834×10^{-5}	90.474148
0.252	49.410	14.617	14.642	0.5293×10^{-2}	90.343
0.26	49.18	14.444	14.657	0.7967×10^{-1}	89.32
0.3	48.1	13.670	14.710	0.3845	84.71
0.32	47.969	13.325	14.724	1.314	82.690
0.33	47.962	13.164	14.729	1.633	81.733
0.34	48.012	13.008	14.733	1.967	80.810
0.5	61.6	11.070	14.730	7.875	69.17
0.6	147	10.192	14.740	11.21	63.61

Table 2: Transition critical values of H together with Ra for various values of ϵ. Porous material Sander sandstone saturated with water. Here $A = 0.395585$ and $\hat{\tau} = 0.1$.

ϵ	H_{trans}	a^2_{stat}	a^2_{osc}	σ^2_1	Ra
0.3	8.19	12.461	8.929	2.571	52.700
0.5	5.97	11.748	10.049	0.3180	48.385
0.7	4.61	10.777	10.365	0.1897×10^{-1}	45.362
0.8	4.205	10.451	10.394	0.3874×10^{-3}	43.984
0.81	4.1853	10.418	10.395	0.2398×10^{-4}	43.844
0.81676471	4.1759	10.395	10.395	0.3074×10^{-5}	43.74816
0.82	4.1727	10.384	10.395	0.6159×10^{-4}	43.702
0.83	4.169	10.350	10.395	0.5354×10^{-3}	43.559
0.84	4.175	10.316	10.394	0.1586×10^{-3}	43.414
0.9	4.81	10.095	10.387	0.4632×10^{-2}	42.486
0.95	231.970	9.872	10.378	0.1282×10^{-1}	41.547

Table 3: Transition critical values of H together with Ra for various values of ϵ. Porous material Aluminium Oxide saturated with water. Here $A = 0.818530$ and $\hat{\tau} = 1$.

ϵ	H_{trans}	Ra	a^2_{stat}	a^2_{osc}
0.4	6.89	50.233	11.906	9.730
0.822279	4.1193	43.643221	10.3766	10.3753
0.83	4.116	43.533	10.3505	10.3757
0.95	95.4	41.534	9.875	10.372

Table 4: Transition critical values for the porous material $AL1050$ saturated with water. The coefficients have values $A = 0.568407543$ and $\hat{\tau} = 1$. These are the transition values occurring in figures 1 - 8.

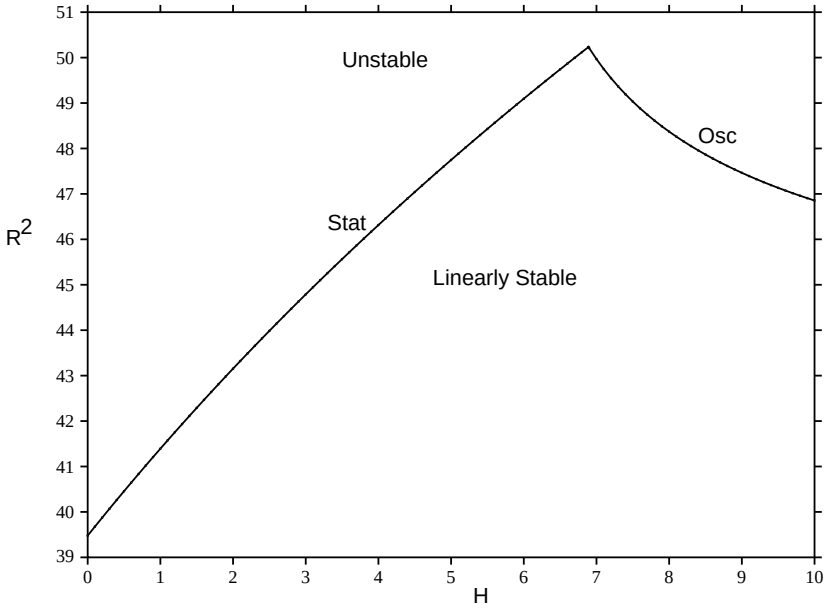

Figure 1: Critical Rayleigh number Ra against H, ϵ has value 0.4. Porous material $AL1050$ saturated with water. Here $A = 0.568407543$ and $\hat{\tau} = 1$.

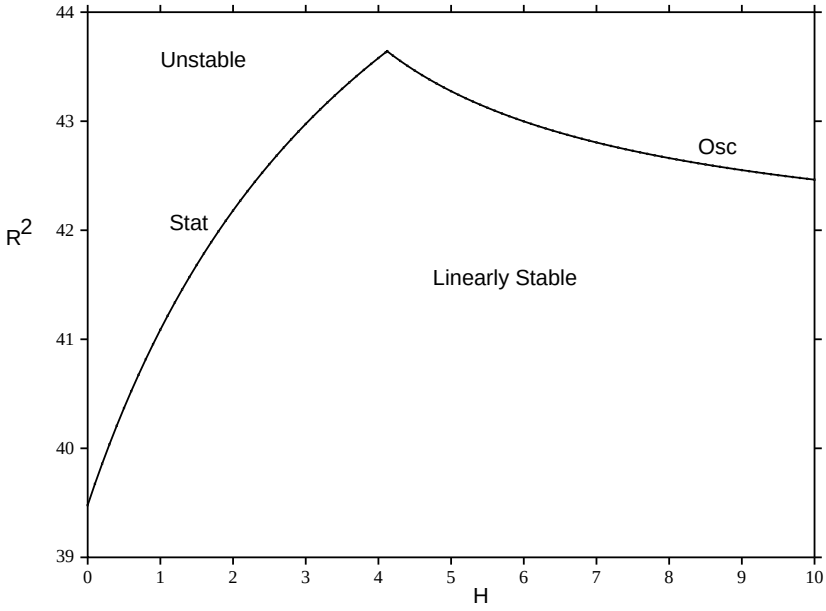

Figure 2: Critical Rayleigh number Ra against H, ϵ has value 0.822279. Porous material $AL1050$ saturated with water. Here $A = 0.568407543$ and $\hat{\tau} = 1$.

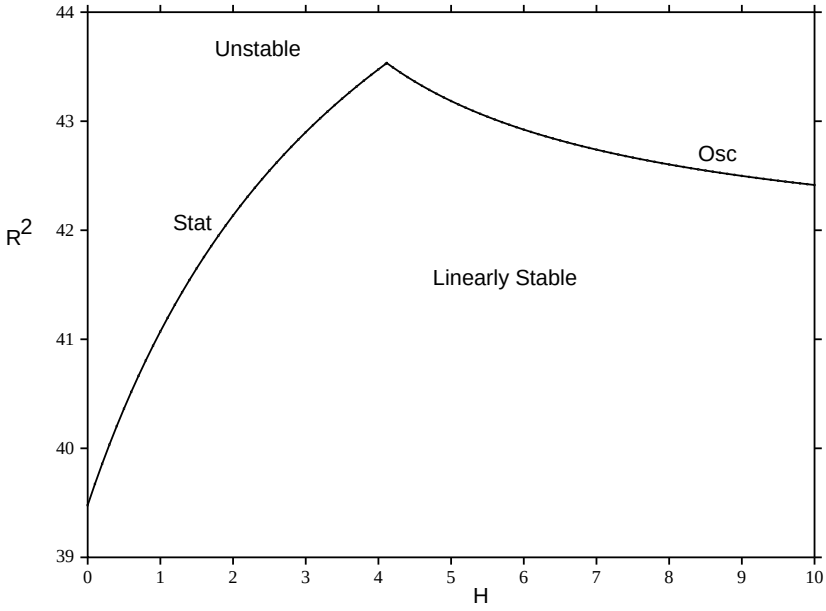

Figure 3: Critical Rayleigh number Ra against H, ϵ has value 0.83. Porous material $AL1050$ saturated with water. Here $A = 0.568407543$ and $\hat{\tau} = 1$.

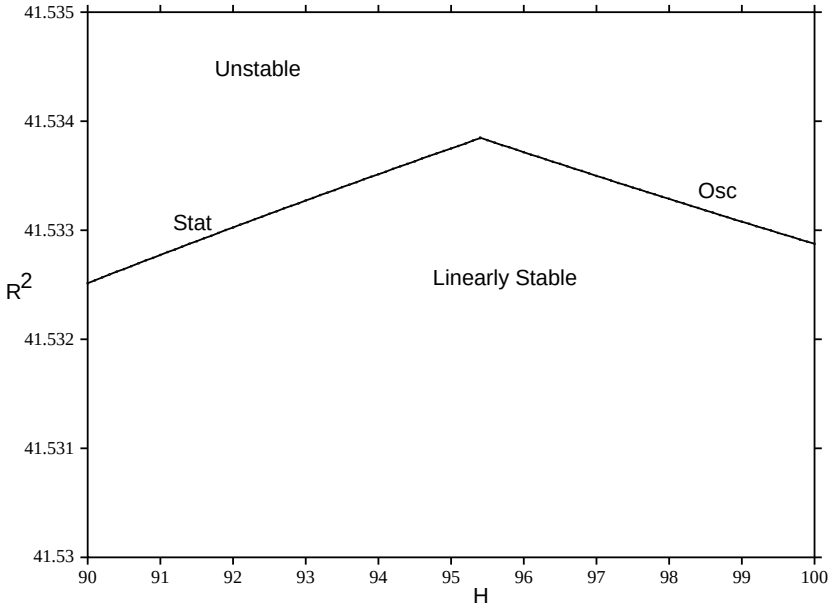

Figure 4: Critical Rayleigh number Ra against H, ϵ has value 0.95. Porous material $AL1050$ saturated with water. Here $A = 0.568407543$ and $\hat{\tau} = 1$.

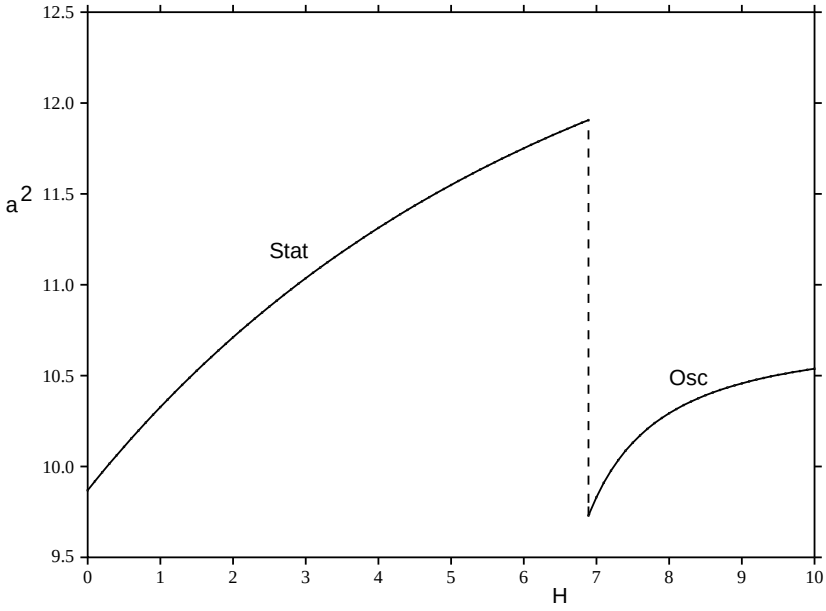

Figure 5: Critical wave number squared a^2 against H, ϵ has value 0.4. Porous material $AL1050$ saturated with water. Here $A = 0.568407543$ and $\hat{\tau} = 1$.

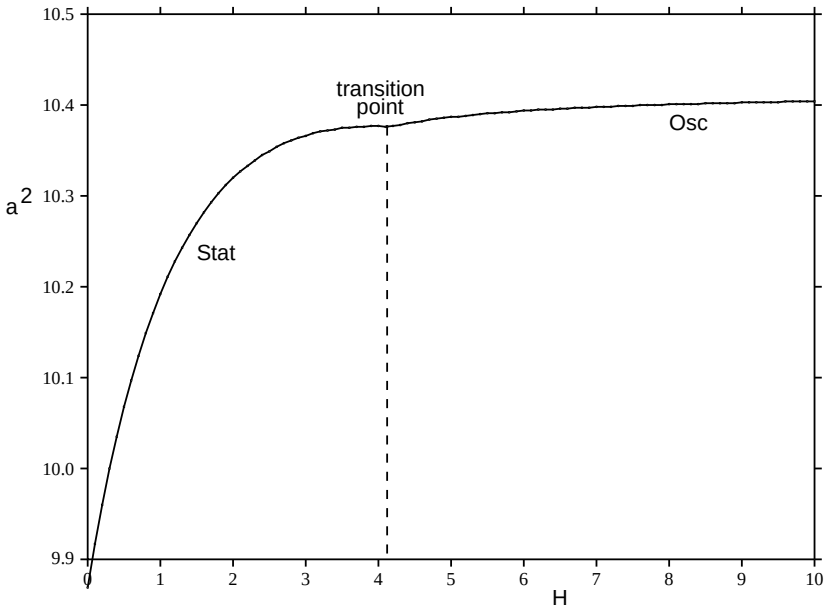

Figure 6: Critical wave number squared a^2 against H, ϵ has value 0.822279. Porous material $AL1050$ saturated with water. Here $A = 0.568407543$ and $\hat{\tau} = 1$.

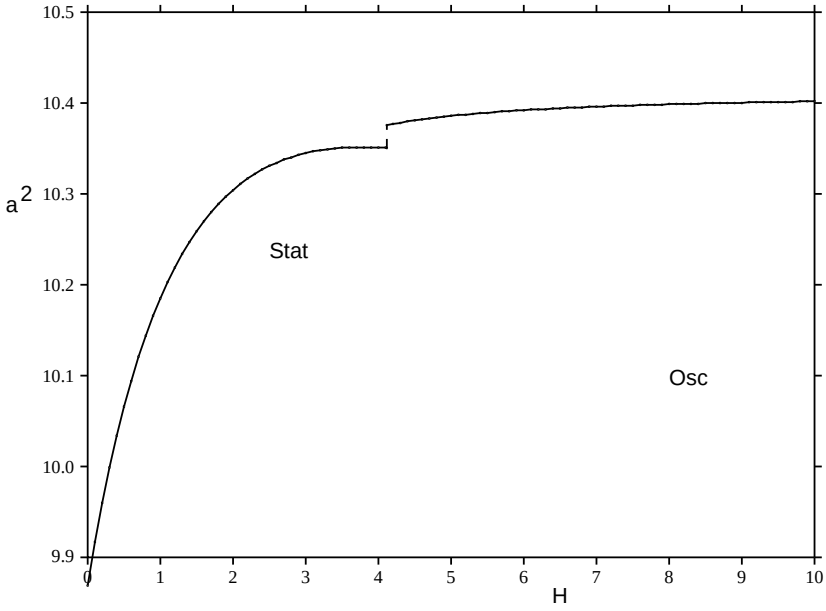

Figure 7: Critical wave number squared a^2 against H, ϵ has value 0.83. Porous material $AL1050$ saturated with water. Here $A = 0.568407543$ and $\hat{\tau} = 1$.

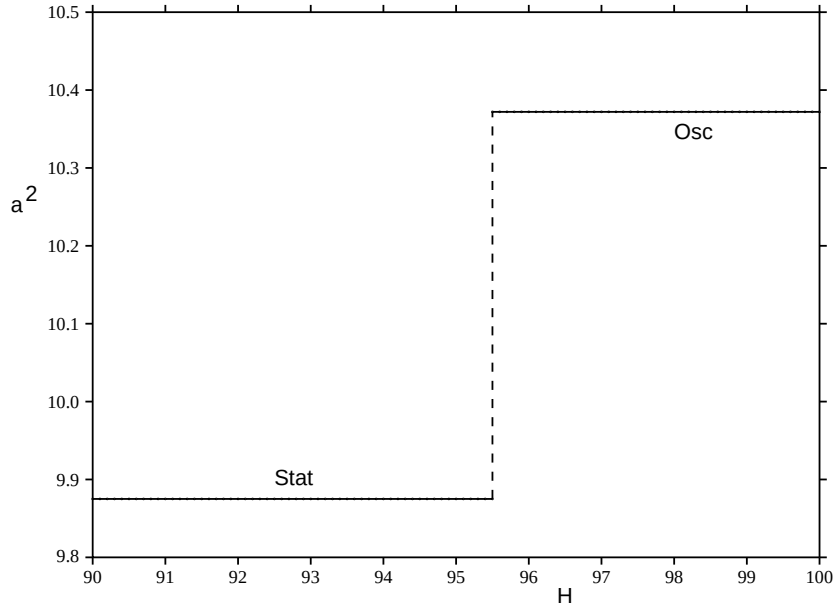

Figure 8: Critical wave number squared a^2 against H, ϵ has value 0.95. Porous material $AL1050$ saturated with water. Here $A = 0.568407543$ and $\hat{\tau} = 1$.